

NEAR-INFRARED TUNABLE BANDPASS FILTERS FOR THE NGST INTEGRATED SCIENCE INSTRUMENT MODULE

M.A. Greenhouse, R. Barclay, S. Satyapal, D., Amato, R. Barry, S. Irish, J. Kuhn, A. Kuttyrev, A. Morell NASA Goddard Space Flight Center, Greenbelt, MD
T. Hilgeman, R. Ryan, L. Lesyna, N. Fonneland Northrop Grumman Corporation, Bethpage, NY

Overview

Demonstrator Unit for Low Order Cryogenic Etalon: DULCE

We display a snap shot of work in progress on near-infrared tunable bandpass filters for the NGST baseline Integrated Science Instrument Module (ISIM) wide field camera. DULCE is designed to demonstrate a high efficiency scanning Fabry-Perot etalon operating in interference orders 1-4 at 30 K with a high stability DSP based servo control system. DULCE has heritage in a Northrop Grumman system designed for 1st order operation at 300 K, and is being developed jointly by GSFC and NGC as a baseline option to satisfy ISIM filter requirements. In this application, scanning etalons will illuminate the focal plane arrays with a single order of interference to enable wide field low resolution ($50 < R < 200$) hyperspectral imaging over a wide range of redshifts.

DULCE cryogenic performance tests will begin in the 3-5 mm range during autumn 1998.

Technology challenge areas:

- high precision long stroke cryogenic actuators
- high stability low drift servo control
- low phase dispersion dielectric multi-layer coatings for 0.6 - 5.3 μm
- etalon plate flatness goal $\sim \lambda/100$ at 30 K after coating ($\lambda = 632 \text{ nm}$)
- mechanical assembly for sub-micron etalon gap at 30 K

DRM Near-Infrared Imaging Requirements Are Enabled By R = 50 - 200 Tunable Filters In Combination With A Small Set of R = 5 Order Sorting Filters

Table 1: Strawman Camera Filter Complement for 1996 DRM

Science	Beam Line Elements	λ (μm)	$\lambda/\Delta\lambda$
Cosmic Distances (core)			
Temporal SN survey	SP1	3.0	1.5
Temporal SN follow up	SP1	3.0	1.5
SN spectroscopy	TBP1[1, 2, 3, 4] + FBP1-7	0.6 - 1.8 tunable	50, 100, 150, 200 selectable
SN spectroscopy	TBP2[1, 2, 3, 4] + FBP1-9	1.8 - 3.0 tunable	50, 100, 150, 200 selectable
SN spectroscopy	TBP3[1, 2, 3, 4] + FBP1-10	3.0 - 4.1 tunable	50, 100, 150, 200 selectable
SN spectroscopy	TBP4[1, 2, 3, 4] + FBP1-11	4.1 - 5.3 tunable	50, 100, 150, 200 selectable
Cosmic Distances			
Gravitational lensing	FBP1-11	0.6 - 5.3	5
Universe at Z > 2 (core)			
Primordial galaxies deep	SP2-5	0.82, 1.43, 2.48, 4.30	2
Primordial galaxies shallow	FBP1-8	0.6 - 2.9	5
Birth of quasars	TBP1[1, 2, 3, 4] + FBP1-7	0.6 - 1.8 tunable	50, 100, 150, 200 selectable
Birth of quasars	TBP2[1, 2, 3, 4] + FBP1-9	1.8 - 3.0 tunable	50, 100, 150, 200 selectable
Birth of quasars	TBP3[1, 2, 3, 4] + FBP1-10	3.0 - 4.1 tunable	50, 100, 150, 200 selectable
Birth of quasars	TBP4[1, 2, 3, 4] + FBP1-11	4.1 - 5.3 tunable	50, 100, 150, 200 selectable
Primordial spectroscopy	FBP1-11	0.6 - 5.3	5
Evolution of galaxies	FBP1-11	0.6 - 5.3	5
Early evolution of galaxies	FBP1-11	0.6 - 5.3	5
Stellar Population			
Local group	FBP1-11	0.6 - 5.3	5
Local group	TBP2[1, 2, 3, 4] + FBP1-9	1.8 - 3.0 tunable	50, 100, 150, 200 selectable
Virgo cluster	FBP1-11	0.6 - 5.3	5
Virgo cluster	TBP2[1, 2, 3, 4] + FBP1-9	1.8 - 3.0 tunable	50, 100, 150, 200 selectable
Solar System			
Planets & asteroids	FBP1-11	0.6 - 5.3	5
Planets & asteroids	TBP1[1, 2, 3, 4] + FBP1-7	0.6 - 1.8 tunable	50, 100, 150, 200 selectable
Planets & asteroids	TBP2[1, 2, 3, 4] + FBP1-9	1.8 - 3.0 tunable	50, 100, 150, 200 selectable
Planets & asteroids	TBP3[1, 2, 3, 4] + FBP1-10	3.0 - 4.1 tunable	50, 100, 150, 200 selectable
Planets & asteroids	TBP4[1, 2, 3, 4] + FBP1-11	4.1 - 5.3 tunable	50, 100, 150, 200 selectable
KBO Survey	FBP1-11	0.6 - 5.3	5
KBO Survey	FBP1-11	0.6 - 5.3	5
KBO follow up	TBP1[1, 2, 3, 4] + FBP1-7	0.6 - 1.8 tunable	50, 100, 150, 200 selectable
KBO follow up	TBP2[1, 2, 3, 4] + FBP1-9	1.8 - 3.0 tunable	50, 100, 150, 200 selectable
KBO follow up	TBP3[1, 2, 3, 4] + FBP1-10	3.0 - 4.1 tunable	50, 100, 150, 200 selectable
KBO follow up	TBP4[1, 2, 3, 4] + FBP1-11	4.1 - 5.3 tunable	50, 100, 150, 200 selectable

Notes:
FBP1 = fixed band pass filter number 1 (see Table 2)
SP1 = special purpose filter number 1 (see Table 2)
TBP1(n) = tunable band pass filter number 1 in order n ($\lambda/\Delta\lambda$ = finesse x order, see Table 3)

Use of Tunable Filters Eases Size Requirement On ISIM Camera Filter Wheels

Fixed Band Pass Filters	Center Wavelength (μm)	FWHM	$\lambda/\Delta\lambda$	Camera Channel	Note
FBP1	0.67	0.14	5	1	
FBP2	0.82	0.17	5	1	
FBP3	1.01	0.21	5	1	
FBP4	1.24	0.26	5	2	
FBP5	1.53	0.32	5	2	
FBP6	1.88	0.39	5	3	
FBP7	2.32	0.46	5	3	
FBP8	2.85	0.59	5	4	
FBP9	3.50	0.72	5	4	
FBP10	4.21	0.89	5	4	
FBP11	4.80	1.0	5	4	

Special Purpose Science Filters	Center Wavelength (μm)	FWHM	$\lambda/\Delta\lambda$	Camera Channel	Note
SP1	3.00	2.00	1.5	1, 2, 3, 4	Temporal SN survey
SP2	0.82	0.14	2	1, 2, 3, 4	Very Deep Field
SP3	1.43	0.17	2	1, 2, 3, 4	Very Deep Field
SP4	2.48	1.24	2	1, 2, 3, 4	Very Deep Field
SP5	4.30	2.07	2	1, 2, 3, 4	Very Deep Field
SP6	0.6 long pass	-	-	3	Grating order sorter
SP7	1.8 long pass	-	-	3	Grating order sorter
Engineering Filters	Beam Stop	-	-	1, 2, 3, 4	Dark Current
E1	Crab	-	-	1, 2, 3, 4	M1 phase capture

Table 3: ISIM Camera Tunable Band Pass Filters

Filter	Total Finesse	Operating Wavelength Range (μm)	Accessible Orders	Camera Channel
TBP1	50	0.6 - 1.04	1-4	1
TBP2	50	1.04 - 1.79	1-4	1
TBP3	50	1.79 - 3.08	1-4	1
TBP4	50	3.08 - 5.32	1-4	1

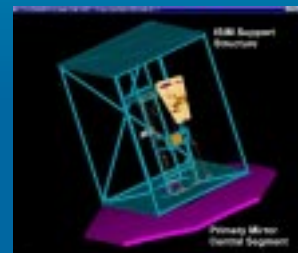
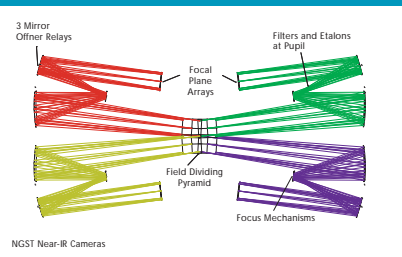
Table 4: ISIM Camera Detector Optimization (μm)

Channel	1.0 - 1.5	1.5 - 2.0	2.0 - 3.0	3.0 - 5.3
Channel 1	1	2	3	4
Channel 2	1	2	3	4
Channel 3	1	2	3	4
Channel 4	1	2	3	4

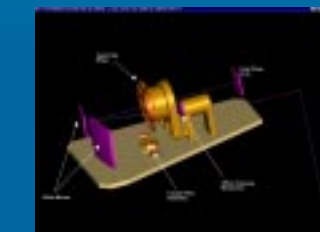
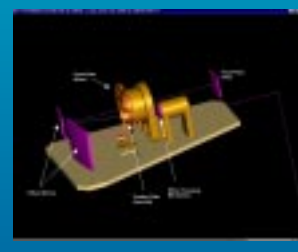
Table 5: Minimum Filter Wheel Capacity

Channel	Positions
1	11
2	11
3	11
4	10

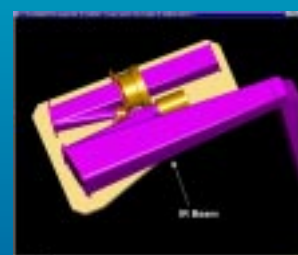
Integrated Science Instrument Module Camera



The ISIM near-infrared wide field camera employs a pyramid beam divider to apportion a 16 square arc-min field of view over four identical camera channels. One channel is shown here in detail. Each channel utilizes a 4096 x 4096 focal plane array covering 4 square arc-min. The baseline ISIM also includes a near-infrared multi-object spectrometer and mid-infrared imaging spectrograph not shown here.

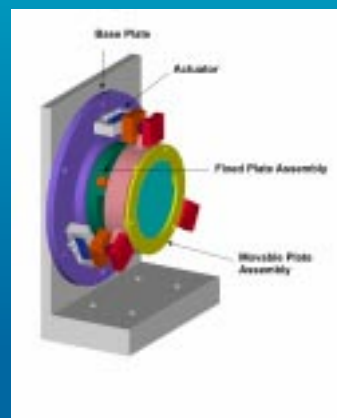


Each camera channel includes a focusing Offner relay, filter wheel, and retractable tunable filter.



The opto-mechanical layout provides sufficient pupil access to accommodate the tunable filter etalon assembly. The etalon shown is 80 mm OD x 40 mm long x 40 mm clear aperture.

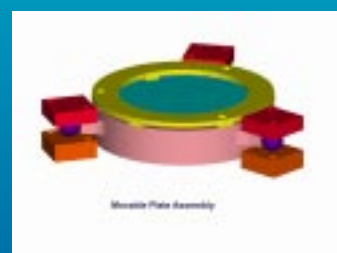
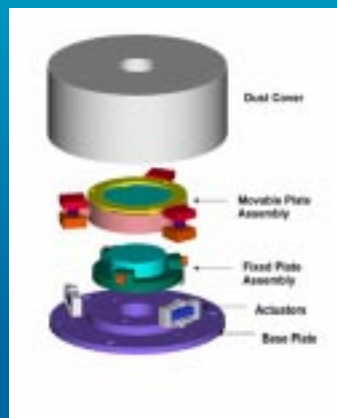
Mechanical Design



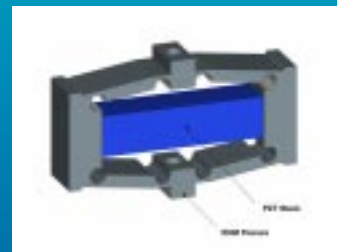
The demonstrator unit plate housings are designed to avoid need for machining details in the plates. This approach reduces cost and facilitates evaluation of a variety of substrates and coatings.



The demonstrator unit plate housings are designed to avoid need for machining details in the plates. This approach reduces cost and facilitates evaluation of a variety of substrates and coatings.



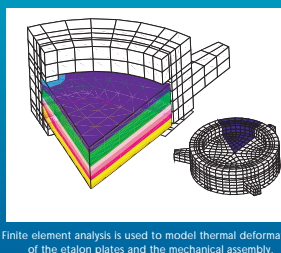
Etalon moving plate assembly with ball bearing kinematic mount. An alternate design utilizing a flexure kinematic mount is also being developed.



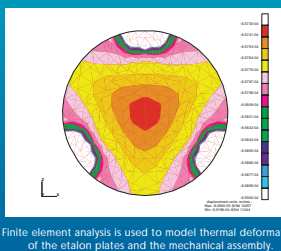
A flexure assembly is used to provide a factor of 8 amplification of the PZT strain.

DULCE

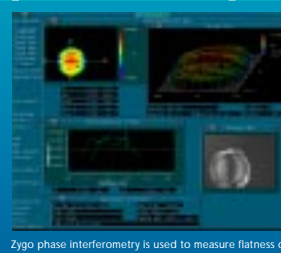
Thermal Modeling



Finite element analysis is used to model thermal deformation of the etalon plates and the mechanical assembly.



Finite element analysis is used to model thermal deformation of the etalon plates and the mechanical assembly.



Zygo phase interferometry is used to measure flatness of the etalon plates and plate/mounting coil assemblies at 30 K.

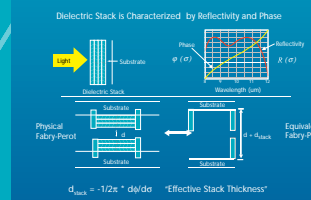
Coating Design

The Effect of Coating Phase Dispersion

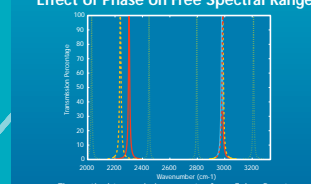
The etalon transmission $T_{\text{eff}}(\theta)$ is given by $T_{\text{eff}}(\theta) = \frac{1}{1 + \frac{4R}{(1-R)^2} \sin^2(\delta)}$ where T and R are the coating transmittance and reflectivity, δ is the phase index of refraction, d is the physical gap length, n is the refractive index of the incident light, θ is the chief ray angle of incidence, θ_0 is the phase shift upon reflection. In the case of dielectric reflectors for which $\theta_0 = 0$, the right hand term does not vanish at $\theta = 0$. In applications requiring low order (near 0) operation, the effective optical thickness of the reflective coating (measured from one) must be taken into account in modeling the effective etalon gap.

Taking a first order Taylor series approximation to $\sin^2(\delta)$ about the center of the bandpass θ_0 , we can write the argument of the sin function as $\delta = \delta_0 + \frac{d}{2} \cos \theta - \frac{d}{2} \cos \theta_0$ where δ_0 is a constant. We define the effective optical thickness of the coating d_{eff} as $d_{\text{eff}} = \frac{1}{2} \frac{d \sin \theta_0}{\cos \theta_0}$ so that $\delta = 2\delta_0 \cos \theta + d_{\text{eff}}(\cos \theta - \cos \theta_0)$. Resonances occur when $\delta = n\pi$, where n is the order of resonance. The order sorting requirement is determined by the wavenumber spacing between successive resonances $\Delta n = \frac{2\pi}{\lambda} \frac{d_{\text{eff}}}{\cos \theta_0}$ and the spectral resolution Δn is $\Delta n = \frac{2\pi}{\lambda} \frac{d_{\text{eff}}}{\cos \theta_0}$ where N_{eff} is the total finesse of the etalon plates. Since the phase dispersion $\frac{d\delta}{d\theta} = -\delta$, Δn is maximized when low phase dispersion coatings are used.

Low-Order Fabry-Perot Interferometer Equivalents



Effect of Phase on Free Spectral Range



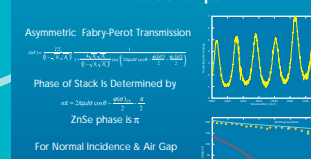
Theoretical transmission spectra for a Fabry-Perot Interferometer ($d=6.7 \mu\text{m}$, $R=95\%$).
- Conventional mirror with no phase control.
- Mirrors with ideal phase characteristics.
- Low-Dispersion mirrors.

Phase Measurements With Fizeau Interferometer



Attributes of Measurement Technique:
• Asymmetric Fabry-Perot
• Simple Mirror Measurement
• ZPS Reference Flat
• No Sophisticated Alignment
• Easy Access to Multiple Orders

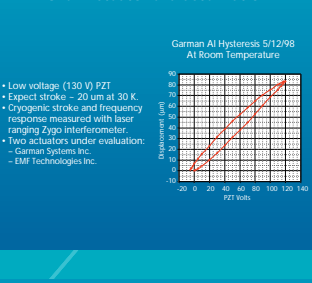
Fizeau Interferometer Relationships



There will be crosstalk between each actuator and each sensor. A translation means will weight contributions from each actuator. The actual strain shown here are just for demonstration. Measurements and analysis are currently on-going.

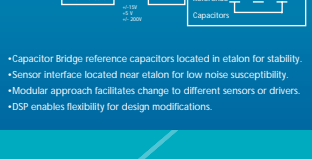
Servo Design

DULCE Actuator Characterization



- Low voltage (130 V) PZT
- Expect stroke $\sim 20 \mu\text{m}$ at 30 K
- Cryogenic stroke and frequency response measured with laser ranging Zygo interferometer.
- Two actuators under evaluation:
- Garman Systems Inc.
- EMI Technologies Inc.

DULCE Electro-Mechanical System Block Diagram



- Capacitor Bridge reference capacitors located in etalon for stability.
- Sensor interface located near etalon for low noise susceptibility.
- Modular approach facilitates change to different sensors or drivers.
- DSP enables flexibility for design modifications.

DULCE Control Electron

- Implemented on TMS320C40 DSP board developed at GSFC.
- Same controller to be used on HIRDLIS magnetic bearing and ZEPHYR wind LIDAR.
- Capacitive sensor demodulation uses lock-in amplifier for high stability and noise rejection. Will provide options for either analog or DSP implementation.
- NGC has demonstrated 0.5 mm rms stability with earlier system.
- 16-bit A/D and D/A converters.
- Capacitor excitation generated digitally on sensor card for high precision and flexibility.

DULCE Electronic Architecture

- Controller Card:**
TMS320C40 DSP, RAM, EEPROM, Actel gate-array, serial interface and parallel digital interface.
- Sensor Card:**
Charge amplifiers, analog lock-in demodulator, A/D converters, D/A converter and EEPROM for capacitor sine-wave excitation generation, selector switch for demodulated or raw signals, multiplexer.
- Driver Card:**
D/A converters, power amplifiers, multiplexer.
- Power Card:**
Power supplies for +/-200V, +/-12V, and +5V.

Control System First-Order Model

